Adsorption (2019) 25:521–528
https://doi.org/10.1007/s10450-019-00024-6

Development of activated graphene-MOF composites for H_2 and CH_4 adsorption

Barbara Szczęśniak[1] · Jerzy Choma[1] · Mietek Jaroniec[2]

Received: 26 December 2018 / Revised: 21 January 2019 / Accepted: 28 January 2019 / Published online: 28 February 2019

Abstract
The structural and adsorption properties of activated graphene/metal–organic framework (MOF) composites are investigated for four samples synthesized by in-situ crystallization and sonication-assisted methods. Depending on the method used, the composites showed different morphology, structure and consequently adsorption properties toward H_2 and CH_4. Addition of KOH-activated graphene during synthesis of an aluminum-containing MOF (MOF520) under sonication conditions boosted adsorption capacities of the resulting composite with respect to both adsorbates, while the in-situ crystallization of MOF520 in mesopores of the CO_2-activated graphene assured very effective coupling of both components. Such comparative study is valuable for the design and synthesis of MOF-based composites for various applications.

Keywords Activated graphene · Graphene-MOF composites · Hydrogen storage · Methane storage · MOF520

1 Introduction

Negative effects of industrial development such as rising energy demands and emission of hazardous gases into atmosphere require immediate solutions. These serious issues can be defused by searching for sustainable energy sources such as CH_4 and H_2, and reducing emissions of greenhouse gases (mainly CO_2), which are produced in large quantities by the industry and other human activities. One of the possible solutions of the issues is the use of nanoporous materials for capture of harmful gases and energy storage applications (Hu et al. 2018; Hedin et al. 2013; Düren 2007; Nishimiya et al. 2002; Siqueira et al. 2017), which nowadays can be designed and synthesized with desired properties.

Metal–organic frameworks (MOFs) are crystalline microporous materials obtained by coordinating metal ions/clusters with appropriate organic ligands. MOFs have received a lot of attention due to tremendous opportunities in tailoring their composition, functionality and structural properties. Some MOFs feature large surface area and pore volume, thus they can exhibit excellent gas adsorption properties (Gándara et al. 2014; Weber et al. 2016; Boutin et al. 2011; Furukawa et al. 2013; Chen et al. 2005). Furthermore, coupling them with carbonaceous materials can provide benefits such as increased thermal stability and water resistance as well as enhanced adsorption properties (Kumar et al. 2013; Szczęśniak et al. 2018; Yang et al. 2014). For instance, graphene oxide (GO) samples can be prepared with high specific surface area, which make them ideal for incorporation into various materials (Szczęśniak et al. 2017; Chen et al. 2017; Zhou et al. 2015b). Moreover, graphene oxide can be modified before its coupling with MOFs. This modification can involve attachment of specific functional groups of high affinity toward organic linkers to increase the number of uncoordinated metal sites in MOF (Policicchio et al. 2013; Lee et al. 2012; Zhao et al. 2013).

In the last several years the properties of graphene-MOF composites have been extensively studied because they represent a very important class of materials with potential applications in adsorption, catalysis, electrochemistry and related areas (Kumar et al. 2014; Liu et al. 2013; Zhou et al. 2015a; Menzel et al. 2016; Huang and Liu 2016; Zhang et al. 2014; Kaur et al. 2017; Banerjee et al. 2015). Various strategies have been reported to prepare graphene-MOF composites, which can be generally divided into in-situ and ex-situ methods. The former is known also as in-situ crystallization (Ji et al. 2017; Szczęśniak et al.

✉ Mietek Jaroniec
jaroniec@kent.edu

[1] Institute of Chemistry, Military University of Technology, 00-908 Warsaw, Poland

[2] Department of Chemistry and Biochemistry, Kent State University, Kent, OH 44-242, USA

2018; Ge et al. 2017; Wang et al. 2016; Qiu et al. 2015; Jin et al. 2016), while the latter are less popular (Xu et al. 2017). The most widely used method, i.e., in-situ crystallization of MOFs on graphene sheets, usually dispersed in a solution, is somehow limited. The main problem is that graphene or graphene-derivative could interact with MOF precursors disturbing its growth. This can lead to a low concentration of MOF, so it is more difficult to control the weight ratio of graphene to MOF in the resulting composites (Szczęśniak et al. 2019). Moreover, the morphology and structure of MOFs and the distribution of each component within composite are also difficult to predict. Thus, the development and improvement of simple and efficient coupling methods would be beneficial for the synthesis of graphene-MOF composites.

In this study we used sonication-assisted method to synthesize activated graphene-MOF composites consisting of activated graphene-derivatives and aluminum-containing MOF520 [$Al_8(OH)_8(BTB)_4(HCOO)_4$, BTB = 4,4′,4″-benzene-1,3,5-triyl-tribenzoate]. For comparison, we also produced analogous composites using in-situ crystallization method. The as-obtained composites were tested as hydrogen and methane adsorbents. MOF520 has been chosen, since it exhibits large specific surface area (above 3000 m^2/g) and high methane storage capacity, i.e., 231 cm^3/cm^3 at 25 °C and 80 bar (Gándara et al. 2014). Activated graphene-derivatives were obtained via KOH and CO_2 activation of 3D (three-dimensional) mesoporous graphene, which was recently reported by our team as a highly efficient benzene adsorbent (Szczęśniak et al. 2019). Although KOH activation process enables the preparation of highly porous carbonaceous materials, including graphene oxide (Klechikov et al. 2015), it significantly deteriorates their structure. In this regard, we propose milder activation procedure (using CO_2) that generates also better structural parameters such as specific surface area and pore volume without damaging 3D network of mesoporous graphene.

2 Experimental

2.1 Chemicals

All chemicals were purchased and used without further purification. They are listed below: graphite powder (99.99%), potassium permanganate (99.5%), hydrogen peroxide (30%), sulfuric acid (95%), orthophosphoric acid (85%), aluminum nitrate nonahydrate (99%), H_3BTB (4,4′,4″-benzene-1,3,5-triyl-tribenzoic acid, 98%), formic acid (80%), *N,N*-dimethylformamide (99.5%), acetone (99.5%), potassium hydroxide (85%), methanol (99.8%) hydrochloric acid (35%).

2.2 Synthesis of activated graphene

Firstly, mesoporous graphene (MG) was prepared by simple exfoliation of graphite oxide at 300 °C in air (Szczęśniak et al. 2019). Carbon dioxide-activated graphene, denoted as GCO_2, was prepared by heating the as-obtained MG at 750 °C in flowing CO_2 for 6 h. To prepare KOH-activated graphene (GKOH), mesoporous graphene was activated using the previously reported procedure (Klechikov et al. 2015).

2.3 Synthesis of activated graphene/MOF composites

The GKOH/MOF-s and GCO_2/MOF-s composites were synthesized by combining aluminum-containing MOF520 [$Al_8(OH)_8(BTB)_4(HCOO)_4$, BTB = 4,4′,4″-benzene-1,3,5-triyl-tribenzoate, denoted as MOF] with GKOH and GCO_2, respectively; using an ultrasonic method; s refers to sonication. Briefly, 0.05 g of activated graphene was dispersed in 5 mL of acetone for 45 min in a closed beaker subjected to ultrasonication. Next, pre-synthesized MOF crystals (according to Gwardiak et al. 2018) were added to assure the graphene:MOF weight ratio 1:2. Subsequently, the mixture was ultrasonically treated for 30 min, and then for additional 15 min in an open beaker to evaporate the solvent. Finally, the composite material was dried at 70 °C. For comparison, GKOH/MOF-c and GCO_2/MOF-c composites were prepared by using the same graphene : MOF weight ratio via in-situ crystallization of MOF on graphene; details of this synthetic method have been reported in our recent study (Szczęśniak et al. 2019). Scheme illustrating route for the synthesis of all activated graphene/MOF composites is shown in Fig. 1.

3 Measurements and calculations

Scanning electron microscopy (SEM), X-ray diffraction analysis (XRD) and nitrogen adsorption were used to characterize the composition, morphology, and structure of the selected samples. The SEM images were performed on a scanning electron microscope LEO 1530 manufactured by Zeiss (Germany) operated at 2 kV acceleration voltage. The XRD analysis was performed on a Bruker D2 PHASER diffractometer with Cu Kα X-rays operating at 30 V and 10 mA. Gas adsorption measurements were carried out using a volumetric adsorption analyzer ASAP 2020 manufactured by Micromeritics Instrument Corp. (Norcross, GA, USA). Each sample was degassed in a vacuum at 150 °C for 12 h prior to adsorption measurements. The specific surface area (S_{BET}) was calculated using the Brunauer–Emmett–Teller

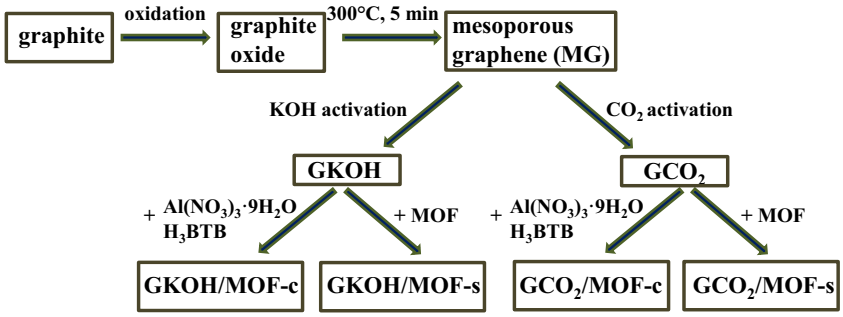

Fig. 1 Scheme illustrating route for the synthesis of activated graphene/MOF composites

method based on nitrogen adsorption isotherms in a relative pressure range of 0.05–0.2. Pore size distributions were determined using the non-local density functional theory method (2D-NLDFT) for carbon slit-shaped pores by taking into account energetic heterogeneity and geometrical corrugation of the surface (Jagiello et al. 2015).

4 Results and discussion

4.1 Structural characterization

Figure 2a shows the SEM image of octahedral crystals of MOF. Figure 2b–d shows that the CO_2 activation preserves the layered 3D interconnected structure of mesoporous graphene (MG) in GCO_2 (Fig. 2d) as opposed to GKOH (Fig. 2c). The latter shows highly defected and rather irregularly shaped structure. Figure 2e–h displays SEM images showing MOF crystals attached to activated graphene sheets. Both GKOH and GCO_2 originate from graphite oxide, thus possess many residual oxygen-containing functional groups. Those groups play an essential role in the formation of graphene-MOF composites, since they can coordinate with aluminum ions from MOF precursors and/or crystals. Apparently, GCO_2 was better merged with MOF crystals due to large (~22.5 nm) mesoporous voids in its layered structure in comparison to GKOH. These mesopores with exposed surface functional groups attached to graphene sheets provide efficient interacting sites for MOF crystals.

Figure 3 shows the XRD pattern of graphite oxide, MG, GCO_2 and GKOH. Characteristic peak of graphite (002) at 26.6° 2 theta shifts to 10.7° 2 theta for graphite oxide due to the combining incorporated oxygen-functional groups and water molecules during the oxidation process of graphite. The (002) peak for MG and GCO_2 are markedly broadened and have a dramatically reduced intensity, which suggest that these materials are largely composed of efficiently separated graphene sheet. A considerable increase in the low-angle scatter from GKOH is associated with the presence of a high density of small pores. Figure 4 displays XRD patterns of MOF and all activated graphene-MOF composites. The characteristic peaks of MOF are in agreement with the earlier report on MOF520, indicating that this material has the structure as expected (Gándara et al. 2014). The XRD patterns of GKOH/MOF-c and GCO_2/MOF-c are a combination of those of the bare MOF and the activated graphene material. While, the patterns of MOF dominate in the patterns of GKOH/MOF-s and GCO_2/MOF-s suggesting the presence of larger MOF crystals. Thus, sonication-assisted method does not provide an efficient way of merging the components into composite as the case of in situ crystallization. The latter method is especially favorable for the preparation of mesoporous graphene/MOF composites since small MOF crystals are formed as evidenced in our recent study (Szczęśniak et al. 2019).

Figure 5 shows low-temperature nitrogen adsorption isotherms measured on mesoporous graphene (MG), and activated graphene materials (GKOH and GCO_2), while Fig. 6 displays isotherms measured on MOF, and activated graphene-MOF composites: GKOH/MOF-c, GCO_2/MOF-c, GKOH/MOF-s, and GCO_2/MOF-s. Figures 7 and 8 show the corresponding pore size distributions (PSD) determined for all samples studied. The nitrogen adsorption isotherms and PSD curves for MG and MOF were published in our previous study of MG/MOF composites (Szczęśniak et al. 2019). KOH-activation of MG with specific surface area S_{BET} = 640 m^2/g and pore volume V_t = 3.03 cm^3/g gave microporous carbon with highly increased surface area S_{BET} (3190 m^2/g) and reduced pore volume V_t (1.81 cm^3/g). In contrast, CO_2 activation of MG resulted in an increase its both S_{BET} and V_t reaching 950 m^2/g and 4.53 cm^3/g, respectively. Surprisingly, CO_2 as a soft activation agent expanded mesoporous structure of the precursor, but basically did not much alter its microporosity unlike in the case of other CO_2-activated carbonaceous materials reported so far (Rasines et al. 2015; Yun et al. 2014). Apparently, the activation process of MG resulted in an additional exfoliation of graphene sheets. Table 1 collects structural parameters calculated for all samples studied. Composites containing GCO_2 showed high total pore volumes reaching 3.11 cm^3/g as well as high S_{BET} up to 2840 m^2/g (GCO_2/MOF-c). The largest S_{BET} = 3100 m^2/g was observed for composite obtained by coupling KOH-activated graphene with MOF via sonication-assisted method (GKOH/MOF-s). This can

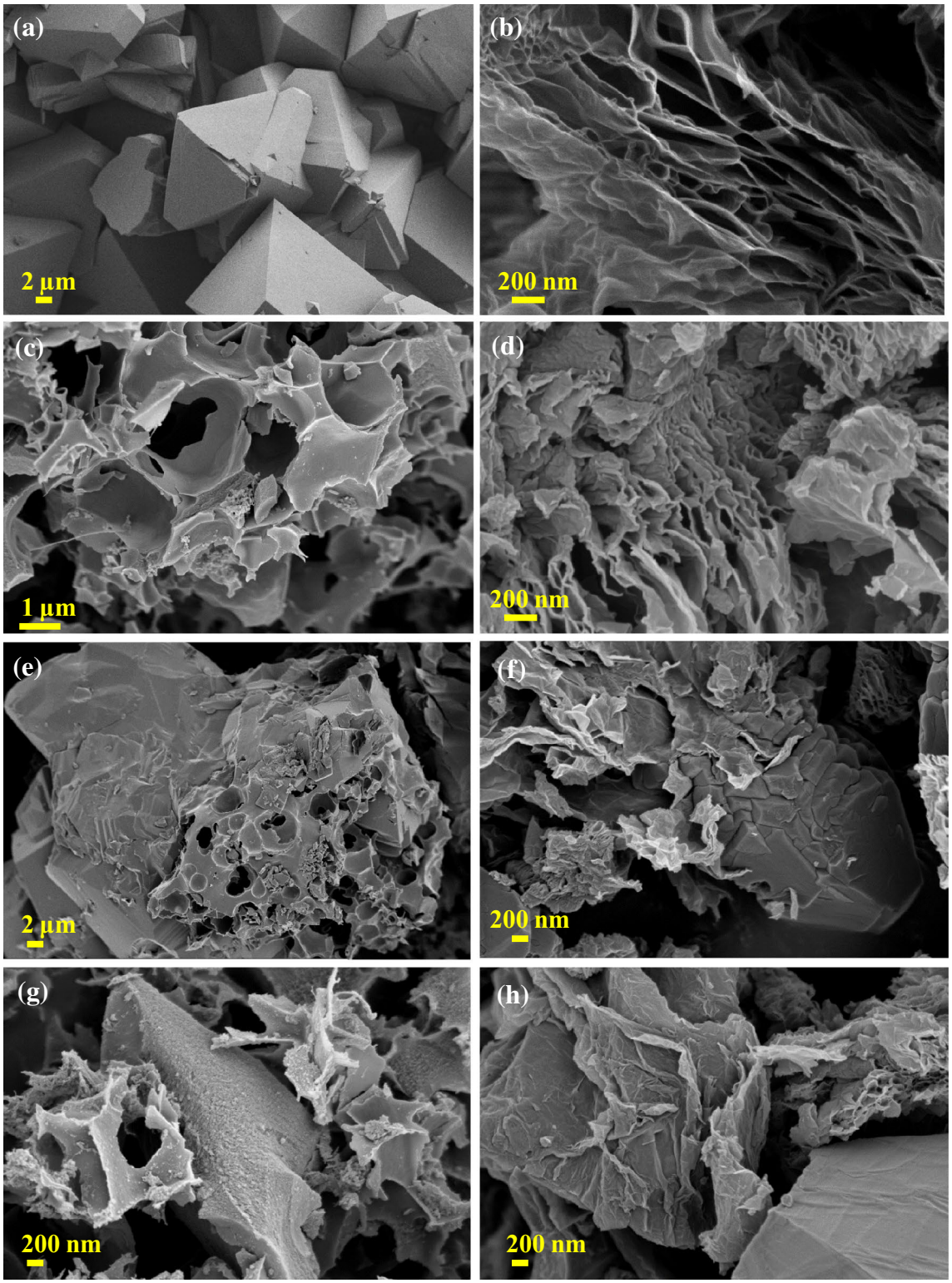

Fig. 2 SEM images of MOF (**a**), MG (**b**), GKOH (**c**), GCO_2 (**d**), GKOH/MOF-c (**e**), GCO_2/MOF-c (**f**), GKOH/MOF-s (**g**) and GCO_2/MOF-s (**h**)

be attributed to the enlarged contact between GKOH and MOF provided by ultrasonication. In contrast, during in situ crystallization process, the presence of MOF precursors may result in the aggregation of GKOH due to the strong attraction between graphene-derived layers.

Apparently, for the synthesis of GCO_2 containing MOF-graphene composites, in situ crystallization method seem to be

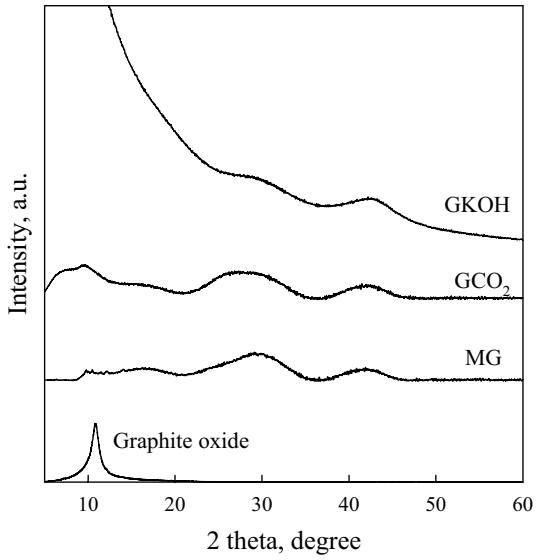

Fig. 3 XRD patterns of graphite oxide, mesoporous graphene and activated graphene materials

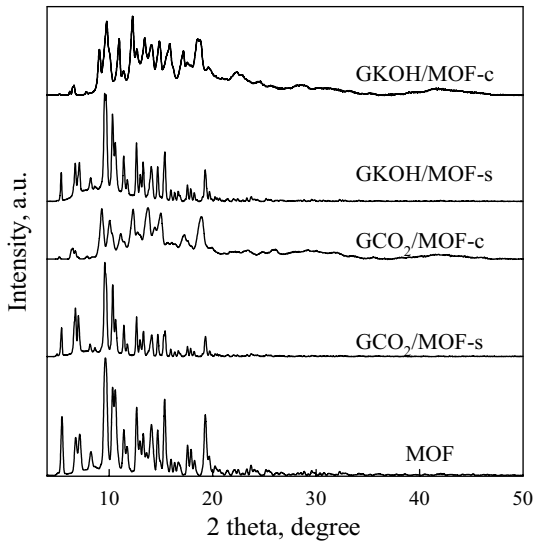

Fig. 4 XRD patterns of MOF and all activated graphene-MOF composites

more adequate, since MOFs can easily grow in the relatively large void spaces between graphene layers. Whereas coupling MOFs with highly microporous carbon materials like GKOH via sonication-assisted method seems to be more efficient due to the better distribution of components.

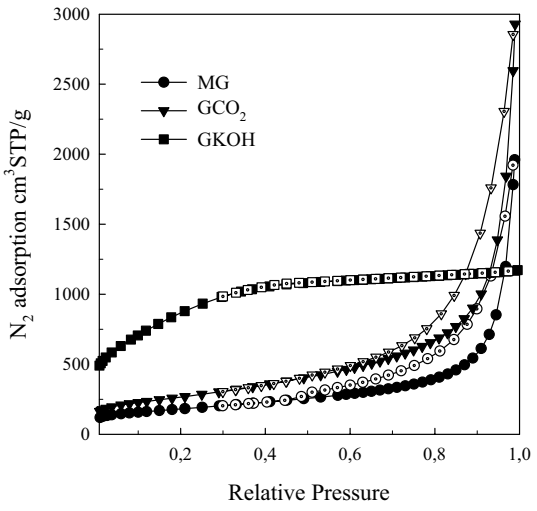

Fig. 5 Low-temperature (− 196 °C) N_2 adsorption–desorption isotherms measured on mesoporous graphene and activated graphene materials

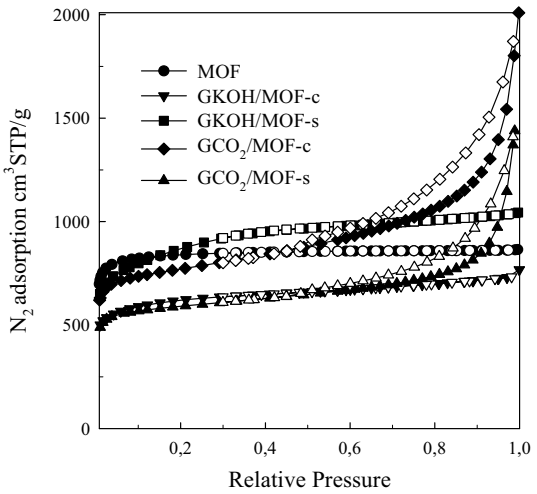

Fig. 6 Low-temperature (− 196 °C) N_2 adsorption–desorption isotherms measured on MOF and activated graphene-MOF composites

5 Adsorption of H_2 and CH_4

The composite obtained by coupling the KOH-activated graphene with MOF using the weight ratio of 1:2 and ultrasound-assisted method (GKOH/MOF-s) adsorbed the highest amount of H_2 at − 196 °C (10.4 mmol/g) and CH_4 at 20 °C (0.83 mmol/g) under 1 bar among all composites studied. These values are higher by 22% and 20%, respectively, in comparison to those on the bare MOF. This enhancement results from the addition of micro-mesoporous activated graphene GKOH that exhibits excellent adsorption properties toward the adsorbates studied.

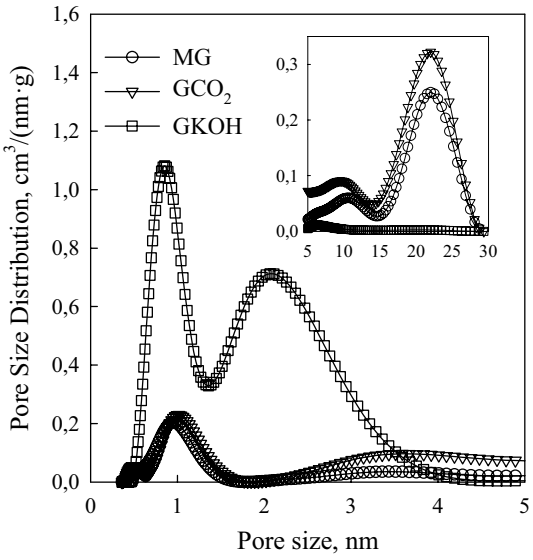

Fig. 7 Differential pore size distributions calculated for mesoporous graphene and activated graphene materials

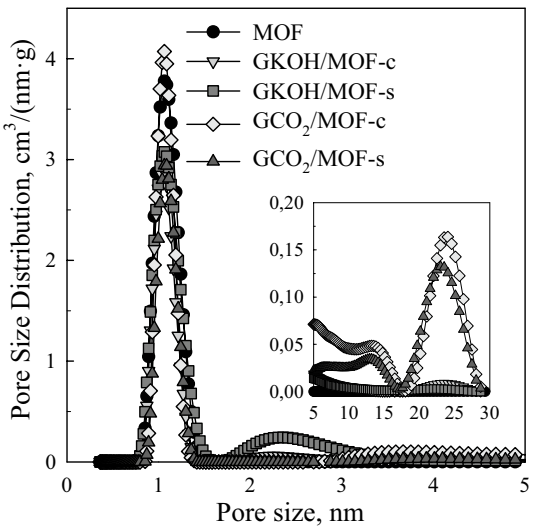

Fig. 8 Differential pore size distributions calculated for MOF and activated graphene-MOF composites

Nevertheless, sonication of the bare MOF (MOF-s) and GKOH (GKOH-s) have a slightly negative influence on the adsorption properties toward H_2 and CH_4 (~5% lower uptakes) (Table 2). Analogues composite obtained by in situ crystallization of MOF in the presence of GKOH (GKOH/MOF-c) showed similar adsorption properties as MOF for both adsorbates, despite lower values of its structural parameters (S_{BET} = 2270 m^2/g, V_t = 1.19 cm^3/g) (Figs. 9, 10). This can be attributed to enhanced interactions between adsorbed molecules and walls of the composite containing GKOH. Contrary, composites with mesoporous additive, i.e., GCO_2/MOF-s and GCO_2/MOF-c showed lower H_2 and CH_4 adsorption capacities in comparison to MOF despite highly enhanced pore volume up to 3.11 cm^3/g. These composites, regardless of the synthesis method used, adsorbed almost the same amounts of both adsorbates, despite quite different values of their structural parameters. The reason for this is that the amount of MOF, which was the same in the both GCO_2/MOF composites, plays a key role in these adsorption processes. Thus, higher mesoporous volume in these materials had no beneficial influence on neither H_2 nor CH_4 adsorption.

Adsorption data obtained for GKOH/MOF-s are competitive to those reported for other solid-state adsorbents. For instance, Zr-containing MOF/GO composite reported recently (Musyoka et al. 2017) adsorbed 9 mmol/g of H_2 at − 196 °C and ~ 1 bar. At the same conditions, graphene oxide without and with Fe_3O_4 nanoparticles adsorbed 8.5 and 10.5 mmol/g of H_2, respectively (Moradi 2015). For

Table 1 Structural parameters of the samples studied

Sorbent	S_{BET} (m^2/g)	V_t (cm^3/g)	V_{micro} (cm^3/g)	Microporosity (%)
MG[a]	640	3.03	0.11	3.6
GCO_2	950	4.53	0.13	2.9
GKOH	3190	1.81	0.93	51.4
MOF[a]	3160	1.34	1.34	100
GKOH/MOF-c	2270	1.19	0.84	70.6
GKOH/MOF-s	3100	1.61	1.11	68.9
GCO_2/MOF-c	2840	3.11	0.97	31.2
GCO_2/MOF-s	2190	2.23	0.77	34.5

S_{BET} BET specific surface area, V_t total (single-point) pore volume obtained from the amount adsorbed at $p/p_0 \approx 0.99$, V_{micro} volume of micropores (pores < 2 nm) obtained on the basis of DFT PSD, *Microporosity* percentage of V_{micro} to the total pore volume (V_t)

[a]Data published in Micropor. Mesopor. Mater. (Szczęśniak et al. 2019)

Table 2 Adsorption uptakes for H_2 and CH_4 at 1 bar on the samples studied expressed in mmol/g

Sorbent	H_2 adsorption (T = − 196°)	CH_4 adsorption (T = 20°)
MOF	8.5	0.69
GCO_2	6.1	0.42
GKOH	14.6	1.54
GKOH/MOF-c	8.6	0.72
GKOH/MOF-s	10.4	0.83
GCO_2/MOF-c	7.1	0.54
GCO_2/MOF-s	7.0	0.54
MOF-s	8.2	0.67
GKOH-s	13.7	1.45

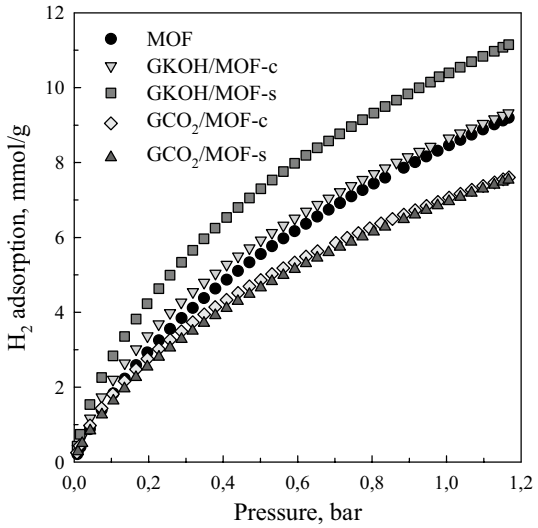

Fig. 9 H_2 adsorption isotherms measured on MOF and its composites with activated graphenes at − 196 °C

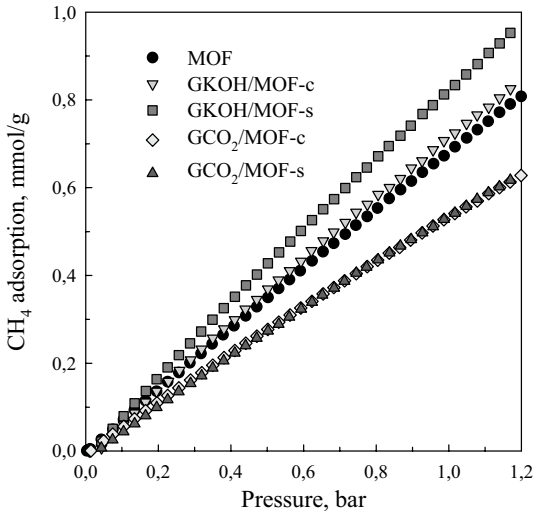

Fig. 10 CH_4 adsorption isotherms measured on MOF and activated graphene-MOF composites at 20 °C

comparison, MOF-5-derived carbon exhibited very high H_2 adsorption capacity, reaching 16.3 mmol/g at − 196 °C and 1 bar (Yang et al. 2012).

6 Conclusions

The aim of this study was to compare the most commonly used methods for the synthesis of graphene-MOF composites i.e., in situ crystallization and sonication-assisted methods. Adsorption capacities for H_2 and CH_4 on the aluminum-containing MOF have been successively improved by incorporation of KOH-activated graphene via sonication-assisted method. This method seem to be more adequate for the preparation of MOF-containing composites with highly microporous carbonaceous additives. Whereas, mesoporous carbons can be efficiently merged with MOFs by in situ crystallization method. Hence, the selection of coupling method for the preparation of graphene-MOF composites is important from the viewpoint of tuning their porous structures and morphology, and consequently adsorption properties.

Acknowledgements BS and JC acknowledge the National Science Centre (Poland) for support of this research under Grant UMO-2016/23/B/ST5/00532.

References

Banerjee, P.C., Lobo, D.E., Middag, R., Ng, W.K., Shaibani, M.E., Majumder, M.: Electrochemical capacitance of Ni-doped metal organic framework and reduced graphene oxide composites: more than the sum of its parts. ACS Appl. Mater. Interfaces **7**, 3655–3664 (2015)

Boutin, A., Couck, S., Coudert, F.-X., Serra-Crespo, P., Kapteijn, F., Alain, H., Fuchs, A.H., Denayer, J.F.M.: Thermodynamic analysis of the breathing of amino-functionalized MIL-53(Al) upon CO_2 adsorption. Micropor. Mesopor. Mater. **140**, 108–113 (2011)

Chen, B., Ockwig, N.W., Millward, A.R., Contreras, D.S., Yaghi, O.M.: High H_2 adsorption in a microporous metal-organic framework with open metal sites. Angew. Chem. **117**, 4823–4827 (2005)

Chen, Y., Lv, D., Wu, J., Xiao, J., Xi, H., Xia, Q., Li, Z.: A new MOF-505@GO composite with high selectivity for CO_2/CH_4 and CO_2/N_2 separation. Chem. Eng. J. **308**, 1065–1072 (2017)

Düren, T.: How does the pore morphology influence the adsorption performance of metal–organic frameworks? A molecular simulation study of methane and ethane adsorption in Zn-MOFs. Stud. Surf. Sci. Catal. **170**, 2042–2047 (2007)

Furukawa, H., Cordova, K.E., O'Keeffe, M., Yaghi, O.M.: The chemistry and applications of metal–organic frameworks. Science **341**, 123044 (1–12) (2013)

Gándara, F., Furukawa, H., Lee, S., Yaghi, O.M.: High methane storage capacity in aluminum metal–organic frameworks. J. Am. Chem. Soc. **136**, 5271–5274 (2014)

Ge, X., Li, Z., Yin, L.: Metal–organic frameworks derived porous core/shell CoP@C polyhedrons anchored on 3D reduced graphene oxide networks as anode for sodium-ion battery. Nano Energy **32**, 117–124 (2017)

Gwardiak, S., Szczęśniak, B., Choma, J., Jaroniec, M.: Benzene adsorption on synthesized and commercial metal–organic frameworks. J. Porous Mat. (2018) https://doi.org/10.1007/s10934-018-0678-0

Hedin, N., Andersson, L., Bergström, L., Yan, J.: Adsorbents for the post-combustion capture of CO_2 using rapid temperature swing or vacuum swing adsorption (review). Appl. Energy **104**, 418–433 (2013)

Hu, X., Brandani, S., Benin, A.I., Willis, R.R.: Testing the stability of novel adsorbents for carbon capture applications using the zero length column technique. Chem. Eng. Res. Des. **131**, 406–413 (2018)

Huang, L., Liu, B.: Synthesis of a novel and stable reduced graphene oxide/MOF hybrid nanocomposite and photocatalytic performance for the degradation of dyes. RSC Adv. **6**, 17873–17879 (2016)

Jagiello, J., Ania, C.O., Parra, J.B., Cook, C.: Dual gas analysis of microporous carbons Using 2D-NLDFT heterogeneous surface model and combined adsorption data of N_2 and CO_2. Carbon **91**, 330–337 (2015)

Ji, D., Zhou, H., Tong, Y., Wang, J., Zhu, M., Chen, T., Yuan, A.: Facile fabrication of MOF-derived octahedral CuO wrapped 3D graphene network as binder-free anode for high performance lithium-ion batteries. Chem. Eng. J. **313**, 1623–1632 (2017)

Jin, Y., Zhao, C., Sun, Z., Lin, Y., Chen, L., Wang, D., Shen, C.: Facile synthesis of Fe-MOF/RGO and its application as a high performance anode in lithium-ion batteries. RSC Adv. **6**, 30763–30768 (2016)

Kaur, R., Kim, K.-H., Deep, A.: A convenient electrolytic assembly of graphene-MOF composite thin film and its photoanodic application. Appl. Surf. Sci. **396**, 1303–1309 (2017)

Klechikov, A., Mercier, G., Sharifi, T., Baburin, I.A., Seifert, G., Talyzin, A.V.: Hydrogen storage in high surface area graphene scaffolds. Chem. Commun. **51**, 15280–15283 (2015)

Kumar, R., Jayaramulu, K., Maji, T.K., Rao, C.N.R.: Hybrid nanocomposites of ZIF-8 with graphene oxide exhibiting tunable morphology, significant CO_2 uptake and other novel properties. Chem. Commun. **49**, 4947–4949 (2013)

Kumar, R., Jayaramulu, K., Maji, T.K., Rao, C.N.R.: Growth of 2D sheets of a MOF on graphene surfaces to yield composites with novel gas adsorption characteristics. Dalton Trans. **43**, 7383–7386 (2014)

Lee, J.H., Kang, S., Jaworski, J., Kwon, K.-Y., Seo, M.L., Lee, J.Y., Jung, J.H.: Fluorescent composite hydrogels of metal–organic frameworks and functionalized graphene oxide. Chem. Eur. J. **18**, 765–769 (2012)

Liu, S., Sun, L., Xu, F., Zhang, J., Jiao, C., Li, F., Li, Z., Wang, S., Jiang, X., Zhou, H., Yang, L., Schick, C.: Nanosized Cu-MOFs induced by graphene oxide and enhanced gas storage capacity. Energy Environ. Sci. **6**, 818–823 (2013)

Menzel, R., Iruretagoyena, D., Wang, Y., Bawaked, S.M., Mokhtar, M., Al-Thabaiti, S.A., Basahel, S.N., Shaffer, M.S.P.: Graphene oxide/mixed metal oxide hybrid materials for enhanced adsorption desulfurization of liquid hydrocarbon fuels. Fuel **181**, 531–536 (2016)

Moradi, S.E.: Enhanced hydrogen adsorption by Fe_3O_4–graphene oxide materials. Appl. Phys. A **119**, 179–184 (2015)

Musyoka, N.M., Ren, J., Langmi, H.W., Northa, B.C., Mathe, M., Bessarabov, D.: Synthesis of rGO/Zr-MOF composite for hydrogen storage application. J. Alloy. Compd. **724**, 450–455 (2017)

Nishimiya, N., Ishigaki, K., Takikawa, H., Ikeda, M., Hibi, Y., Sakakibara, T., Matsumoto, A., Tsutsumi, K.: Hydrogen sorption by single-walled carbon nanotubes prepared by a torch arc method. J. Alloys Compd. **339**, 275–282 (2002)

Policicchio, A., Zhao, Y., Zhong, Q., Agostino, R.G., Bandosz, T.J.: Cu-BTC/aminated graphite oxide composites as high-efficiency CO_2 capture media. ACS Appl. Mater. Inter. **6**, 101–108 (2013)

Qiu, X., Wang, X., Li, Y.: Controlled growth of dense and ordered metal–organic framework nanoparticles on graphene oxide. Chem. Commun. **51**, 3874–3877 (2015)

Rasines, G., Macías, C., Haro, M., Jagiello, J., Ania, C.O.: Effects of CO_2 activation of carbon aerogels leading to ultrahigh micro-meso porosity. Microporous Mesoporous Mater **209**, 18–22 (2015)

Siqueira, R.M., Freitas, G.R., Peixoto, H.R., Nascimento, J.F., Musse, A.P.S., Torres, A.E.B., Azevedo, D.C.S., Bastos-Neto, M.: Carbon dioxide capture by pressure swing adsorption. Energy Proc **114**, 2182–2192 (2017)

Szczęśniak, B., Choma, J., Jaroniec, M.: Gas adsorption properties of graphene-based materials. Adv. Colloid Interface Sci. **243**, 46–59 (2017)

Szczęśniak, B., Choma, J., Jaroniec, M.: Gas adsorption properties of hybrid graphene-MOF materials. J. Colloid Interface Sci. **514**, 801–813 (2018)

Szczęśniak, B., Choma, J., Jaroniec, M.: Ultrahigh benzene adsorption capacity of graphene-MOF composite fabricated via MOF crystallization in 3D mesoporous graphene. Micropor. Mesopor. Mater. **279**, 387–394 (2019)

Wang, Y., Zhang, W., Wu, X., Luo, C., Liang, T., Yan, G.: Metal-organic framework nanoparticles decorated with graphene: a high-performance electromagnetic wave absorber. J. Magn. Magn. Mater. **416**, 226–230 (2016)

Weber, G., Bezverkhyy, I., Bellat, J.-P., Ballandras, A., Ortiz, G., Chaplais, G., Patarin, J., Coudert, F.X., Fuchs, A.H., Boutin, A.: Mechanism of water adsorption in the large pore form of the gallium-based MIL-53 metal-organic framework. Microporous Mesoporous Mater **222**, 145–152 (2016)

Xu, X., Shi, W., Li, P., Ye, S., Ye, C., Ye, H., Lu, T., Zheng, A., Zhu, J., Xu, L., Zhong, M., Cao, X.: Facile fabrication of three-dimensional graphene and metal–organic framework composites and their derivatives for flexible all-solid-state supercapacitors. Chem. Mater. **29**, 6058–6065 (2017)

Yang, S.J., Kim, T., Im, J.H., Kim, Y.S., Lee, K., Jung, H., Park, C.R.: MOF-derived hierarchically porous carbon with exceptional porosity and hydrogen storage capacity. Chem. Mater. **24**, 464–470 (2012)

Yang, Y., Ge, L., Rudolph, V., Zhu, Z.: In situ synthesis of zeolitic imidazolate frameworks/carbon nanotube composites with enhanced CO_2 adsorption. Dalton Trans. **43**, 7028–7036 (2014)

Yun, S., Kang, S.O., Park, S., Park, H.S.: CO_2-activated, hierarchical trimodal porous graphene frameworks for ultrahigh and ultrafast capacitive behavior. Nanoscale **6**, 5296–5302 (2014)

Zhang, Y., Li, G., Lu, H., Lv, Q., Sun, Z.: Synthesis, characterization and photocatalytic properties of MIL-53(Fe)–graphene hybrid materials. RSC Adv. **4**, 7594–7600 (2014)

Zhao, Y., Seredych, M., Zhong, Q., Bandosz, T.J.: Aminated graphite oxides and their composites with copper-based metal–organic framework: in search for efficient media for CO_2 sequestration. RSC Adv. **3**, 9932–9941 (2013)

Zhou, H., Zhang, J., Zhang, J., Yan, X.-F., Shen, X.-P., Yuan, A.-H.: Spillover enhanced hydrogen storage in Pt-doped MOF/graphene oxide composite produced via an impregnation method. Inorg. Chem. Commun. **54**, 54–56 (2015a)

Zhou, X., Huang, W., Miao, J., Xia, Q., Zhang, Z., Wang, H., Li, Z.: Enhanced separation performance of a novel composite material GrO@MIL-101 for CO_2/CH_4 binary mixture. Chem. Eng. J. **266**, 339–344 (2015b)